



Mineralogy and carbonate geochemistry of the Dali Lake sediments: Implications for paleohydrological changes in the East Asian summer monsoon margin during the Holocene

Jiawei Fan ^{a, b, *}, Jule Xiao ^{a, b, c}, Ruilin Wen ^{a, b}, Shengrui Zhang ^{a, b}, Yun Huang ^{a, b}, Jiaojiao Yue ^{a, b}, Xu Wang ^{a, b}, Linlin Cui ^{a, b}, He Li ^d, Dingshuai Xue ^d, Yanhong Liu ^d

^a Key Laboratory of Cenozoic Geology and Environment, Institute of Geology and Geophysics, Chinese Academy of Sciences, Beijing 100029, China

^b Institutions of Earth Science, Chinese Academy of Sciences, Beijing 100029, China

^c College of Earth Sciences, University of Chinese Academy of Sciences, Beijing 100049, China

^d State Key Laboratory of Lithospheric Evolution, Institute of Geology and Geophysics, Chinese Academy of Sciences, Beijing 100029, China

ARTICLE INFO

Article history:

Received 24 October 2017

Received in revised form

17 March 2018

Accepted 18 March 2018

Available online 26 March 2018

Keywords:

Dali lake

Mineralogy

Carbonate geochemistry

Paleohydrological change

East asian summer monsoon

Holocene

ABSTRACT

Hydrological variations in individual plateau lakes respond from both local hydrological processes and regional climatic changes. This study presents high resolution, absolutely-dated records of minerals in bulk samples and elements and stable isotopes of endogenic calcites from a sediment core from Dali Lake in Inner Mongolian Plateau, aiming to investigate the patterns and mechanisms of Holocene hydrological and climatic changes in the modern northern margin of the East Asian summer monsoon (EASM). Increases in the percentages of allogenic minerals (quartz, microcline and albite) and decreases in the percentages of endogenic/authigenic minerals (calcite, Mg-calcite and gypsum), together with decreases in the values of Ca and Mg concentrations and $\delta^{18}\text{O}$ and $\delta^{13}\text{C}$ of endogenic calcites indicate an excess of water input to the lake over evaporative losses, and vice versa. These data suggest that the hydrological balance of Dali Lake was controlled by strong evaporation before 9800 cal yr BP, and then the lake was supplied by significantly increased inflowing water between 9800 and 5900 cal yr BP. From 5900 to 4850 cal yr BP, the water input to the lake significantly decreased. Since 4850 cal yr BP, the inflowing water maintained a low level. In addition, the distinct characteristics of mineralogy and carbonate geochemistry of the Dali Lake sediments during the periods of high lake level between 9800–7700 and 7700–5900 cal yr BP imply that the lake was mainly fed by snow/ice melt water in the former period and then by regional precipitation in the latter period, which was further supported by the pollen records from the same sediment core. These results suggest that Holocene hydrological variations in the EASM margin were closely related to changes in regional temperature and precipitation which were ultimately controlled by changes in the Northern Hemisphere summer insolation, northern high latitude ice sheets, global sea level and physicochemical conditions of the North Atlantic and western tropical Pacific on orbital and millennial timescales. The datasets in this study support that the maximum EASM intensity occurred during the middle Holocene in the northern EASM regions.

© 2018 Elsevier Ltd and INQUA. All rights reserved.

1. Introduction

The East Asian summer monsoon (EASM), an integral component of the global climate system, plays a key role in transporting heat and moisture from low to high latitudes (An, 2000). On the

regional scale, the livelihood of dense populations in the EASM regions is closely related to the monsoonal precipitation; however, recurrent flooding or severe drought brings serious challenges for the human society due to the large variability of the EASM.

During the last two decades, a variety of paleoclimatic records have been reported to understand the nature of Holocene Asian monsoon variations on various timescales and the underlying forcing mechanisms (Xiao et al., 2004; Dykoski et al., 2005; Wang et al., 2005; Porter and Zhou, 2006; Chen et al., 2008; An et al.,

* Corresponding author. Institutions of Earth Science, Chinese Academy of Sciences, Beijing 100029, China.

E-mail address: jwfan@mail.iggcas.ac.cn (J. Fan).

2012; Li et al., 2017a; Zhong et al., 2017; Zhang et al., 2018). Their results suggest asynchronous Holocene Asian monsoon intensification in different regions (An et al., 2000; Xiao et al., 2004; Chen et al., 2015; Cheng et al., 2016; Li et al., 2017b). For example, high-resolution, absolutely dated oxygen isotope records of stalagmites from Dongge Cave (Wang et al., 2005; Dykoski et al., 2005) and Daoguan Cave (Liu et al., 2017) in southern China indicate that the Asian summer monsoon intensified significantly at 11,000–10,000 yr BP, reached the maximum level during the early to middle Holocene, and then decreased at 7000–6500 yr BP. By contrast, pollen records from Daihai Lake (Xiao et al., 2004), Hulun Lake (Wen et al., 2010), Dali Lake (Xiao et al., 2015; Wen et al., 2017) and Gonghai Lake (Chen et al., 2015) in northern China suggest that the EASM did not significantly intensify until 8000 cal yr BP, maintained a high intensity during the middle Holocene, and then weakened at 6000–5000 cal yr BP. However, such viewpoint of spatial differences of maximum monsoon intensification was rejected by Goldsmith et al. (2017), based on their inference of high water level of Dali Lake during the early and middle Holocene evidenced from six optical stimulated luminescence (OSL) samples and sixteen radiocarbon dating samples from lake sediments, alluvial deposits and beach ridges; while records of paleoclimate from individual lakes respond from both local and regional events, especially for those plateau lakes that collect water from both snow/ice melt in the lake catchment and atmospheric precipitation during the geological past (Zhou et al., 2016; Zhang et al., 2017).

Dali Lake is located in the central-eastern Inner Mongolian Plateau (Fig. 1). The major inflow of Dali Lake, the Gongger River, originates from the Great Hinggan Mountains, discharges melt water during spring floods as large as during summer floods (Li, 1993), which implies that the snow/ice melt water may have made great contributions to the high water level of Dali Lake during the early Holocene when large areas of ice sheets over northern high latitudes rapidly melted and retreated (Dyke, 2004; Carlson et al., 2008; Parducci et al., 2012). In this study, we present precisely AMS ^{14}C dated records of minerals in bulk samples and elements and stable isotopes of endogenic calcites from a sediment core recovered in the depo-center of Dali Lake. The main aim is to use these new datasets to identify the different characteristics of high water level of Dali Lake between early and middle Holocene, and to investigate the possible forcing mechanisms for these two different periods of high lake level. These data may improve our understanding of the Holocene monsoon variations in the northern EASM regions.

2. Regional setting

Dali Lake ($43^{\circ}13'–43^{\circ}23'$ N, $116^{\circ}29'–116^{\circ}45'$ E) is an inland closed-basin lake in the central-eastern Inner Mongolian Plateau (Fig. 1). The lake has an area of 238 km², a maximum water depth of 11 m and an elevation of 1226 m above sea level. Hills of basaltic rocks surround the lake to the north and west, and lacustrine plains are present along the eastern shore, and there is no outcrop of gypsum and carbonate rocks in the region. Four rivers enter the lake (Fig. 1), among which the Gongger River, the major inflow, originates from the southern terminal part of the Great Hinggan Mountains, where the elevation reaches 2029 m, supplies 75% of the total inflowing water (Li, 1993).

Dali Lake sits at the northern margin of the EASM (An, 2000). The area has a mean annual temperature is 3.2 °C with a July average of 20.4 °C and a January average of –16.6 °C (Fan et al., 2016). Mean annual precipitation is 383 mm with ~70% of the annual precipitation falling in June–August (Fan et al., 2016). Mean annual evaporation reaches 1632 mm (Fan et al., 2016). The lake is covered with ice from early November to late April.

The water of Dali Lake at present is alkaline and brackish, and contains major cations of Ca^{2+} (5.5 mg/l), Mg^{2+} (33.7 mg/L), K^{+} (266.3 mg/L) and Na^{+} (2516.7 mg/L), and major anions of CO_3^{2-} (644.3 mg/L), HCO_3^{-} (2336.0 mg/L), SO_4^{2-} (403.0 mg/L) and Cl^{-} (1753.3 mg/L) (Fan et al., 2016). The average value of $\text{Mg}^{2+}/\text{Ca}^{2+}$ mole ratio of lake water is 8.3. The $\delta^{18}\text{O}$ and δD values of lake water average –2.1‰ (VSMOW) and –22.5‰ (VSMOW), respectively, while the $\delta^{13}\text{C}_{\text{DIC}}$ averages –0.3‰ (PDB) (Fan et al., 2016). The inflowing water of Gongger River has an average $\text{Mg}^{2+}/\text{Ca}^{2+}$ mole ratio of 0.52, average $\delta^{18}\text{O}$ and δD values of –13.1‰ (VSMOW) and –94.5‰ (VSMOW), respectively, and an average $\delta^{13}\text{C}_{\text{DIC}}$ value of –7.8‰ (PDB) (Fan et al., 2016).

3. Material and methods

The upper 8.5 m of the DL04 sediment core recovered from the depocenter of the Dali Lake ($43^{\circ}15.68'$ N, $116^{\circ}36.26'$ E) (Fig. 1) is used for the present study. The coring method was described in Xiao et al. (2008) and the lithology was described in Fan et al. (2017).

Fifteen bulk samples from the organic-rich horizons from the upper 8.5 m of the DL04 core were radiocarbon dated using an Accelerator Mass Spectrometry (AMS) system (Compact-AMS, NEC Pelletron) at the Paleo Labo Co., Ltd (Japan). The dating method was described in Xiao et al. (2008). The chronological results and the age–depth model of the DL04 core were presented in Fan et al. (2017). The upper 8.5 m of the DL04 core covered the last 11,500 yr.

The sediments from the upper 8.5 m of the DL04 core are sampled at 1- to 6-cm intervals (~50-yr resolution), yielding a total of 221 samples for mineral analyses. The composition and percentage of minerals are determined with a Rigaku D/MAX–2400 X-ray diffractometry (XRD) equipped with a graphite monochromator. Each sample is spread and leveled onto a $2 \times 1.5 \text{ cm}^2$ concave glass plate for determinations with the XRD. The XRD employs the radiation of a Cu target at 40 KV, 60 mA to generate X ray that irradiates a sample at a scanning angle of 2θ ($2\theta = 3^{\circ}–70^{\circ}$) and produces the diffraction peaks of the sample. These peaks are filtered and monochromatized through the graphite monochromator, resulting in the characteristic diffraction peaks of minerals comprising the sample. The composition of minerals in a sample are determined by comparison of the sample's characteristic diffraction peaks with the standard card spectrum, and the relative percentages are calculated by the proportions of the integral intensity (peak width at half height multiplied by peak height) of the characteristic diffraction peaks of each minerals using the software MDI Jade 6. The relative error of percentages of the related minerals in a sample is less than 3%. In addition, four representative sediment samples are sieved through a 400-mesh (38- μm pore size) sieve to obtain the <38- μm fractions and the <38- μm carbonates in these sediments are used for the scanning electron microscope (SEM) analyses with a LEO1450VP SEM.

The sediments from the carbonate-rich horizons of the DL04 core are sampled at 1- to 6-cm intervals, yielding a total of 173 samples for analyses of Ca and Mg concentrations, Mg/Ca ratio, and oxygen and carbon isotope composition of the carbonates. Each sample of ~500 mg of air-dried bulk sediments are sieved through a 400-mesh (38- μm pore size) sieve to obtain the <38- μm sediments. Concentrations of Ca and Mg of the carbonates in <38- μm sediments are determined with an ICP-OES using the method described in Fan et al. (2016). Mg/Ca mole ratio is calculated by its mass ratio times a coefficient of 1.67. $\delta^{18}\text{O}$ and $\delta^{13}\text{C}$ values of the <38- μm carbonates are determined with a Finnigan MAT 253 mass spectrometer equipped with a Gas Bench–II carbonate preparation device, using the method described in Fan et al. (2016).

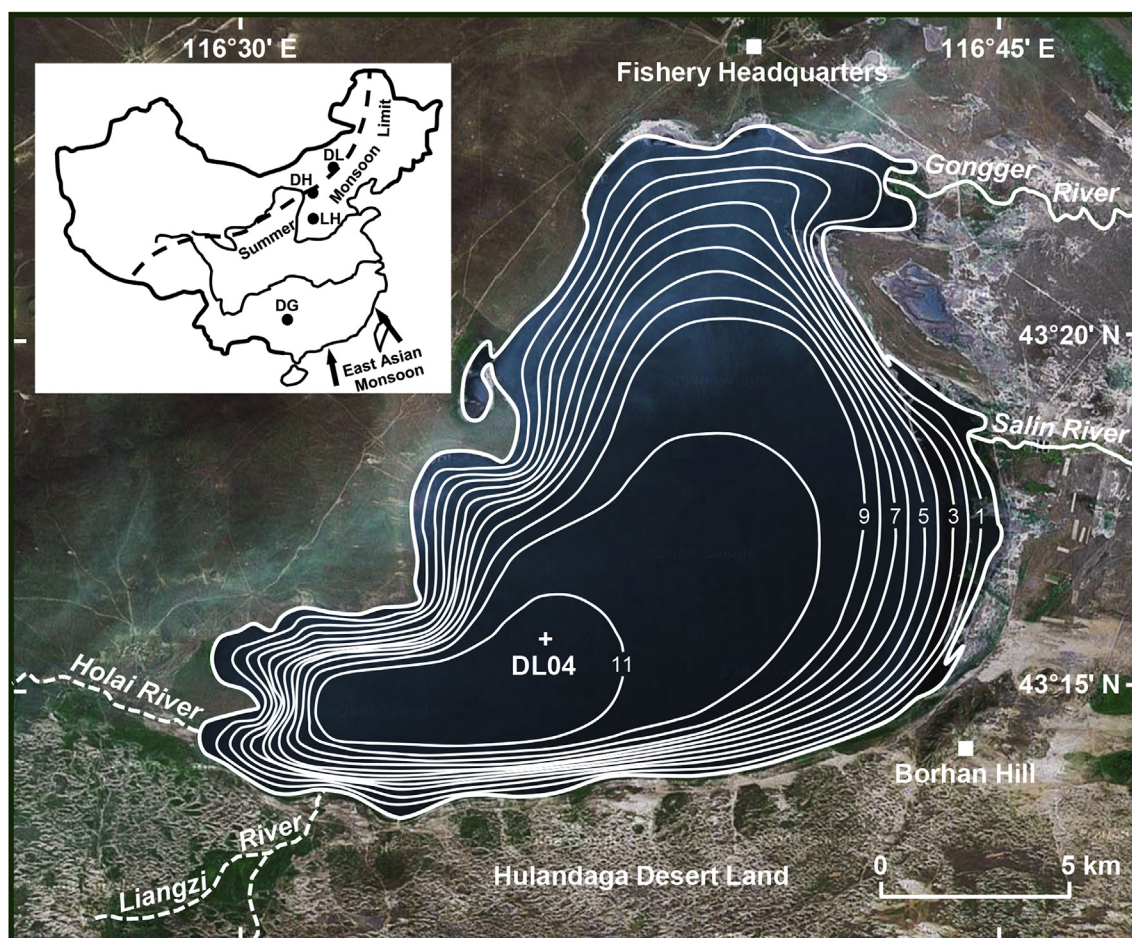


Fig. 1. Map of Dali Lake (from <http://maps.google.com>) showing the location of the DL04 sediment core (cross). The bathymetric survey of the lake was conducted in June 2002 using a FE-606 Furuno Echo Sounder (contours in m). The inset map shows the locations of Dali Lake (DL; 43°15' N, 116°36' E), Daihai Lake (DH; 40°35' N, 112°40' E), Lianhua Cave (LH; 38°10' N, 113°43' E) and Dongge Cave (DG; 25°17' N, 108°5' E) and the modern northern limit of the East Asian summer monsoon defined by the 400-mm isohyet of mean annual precipitation (Xiao et al., 2004).

4. Results

The XRD results show that the major minerals in bulk sediments from the upper 8.5 m of the DL04 core are consist of quartz, microcline, albite, illite, clinochlore, gypsum, calcite and Mg-calcite (Fig. 2). Other minerals (such as apatite in Fig. 2B) are relatively less. The calcite and Mg-calcite crystals in <38- μ m sediments are granular, blocky, lenticular and prismatic idiomorphic, and generally <10 μ m in grain size (Fig. 3). The time series of mineral percentages in bulk sediments, and elements and stable isotope composition of <38- μ m calcites spanning the last 11,500 cal yr can be generally divided into three stages (Fig. 4), as follows:

4.1. Stage 3 (850–763 cm, 11,500–9800 cal yr BP)

This stage is characterized by relatively low percentages of quartz, albite and clinochlore and high percentages of gypsum and calcite, as well as high values of Ca and Mg concentrations, Mg/Ca ratios and $\delta^{18}\text{O}$ and $\delta^{13}\text{C}$. Quartz percentages average 50.3% with their minimum of 36.8% at 10,970 cal yr BP; microcline percentages average 8.0% with their maximum of 18.6% at 10,970 cal yr BP; albite, illite and clinochlore percentages average 9.7%, 3.5% and 2.5%, respectively. Gypsum percentages average 3.5% with their maximum of 8.4% at 10,930 cal yr BP and calcite percentages average 23.5% with their maximum of 38.0% at 10,120 cal yr BP.

The elements and stable isotope composition show high values in this stage. Both Ca and Mg concentrations exhibit decreasing trends with trough values of 0.4% and 0.17%, respectively, at 10,680 cal yr BP and high peaks of 4.9% and 1.25% at 11,050 cal yr BP. Mg/Ca ratios average 0.40 with a peak of 0.65 at 10,680 cal yr BP. $\delta^{18}\text{O}$ and $\delta^{13}\text{C}$ values vary within overall ranges of -6.1‰ to -2.9‰ and 0.9‰ – 3.3‰ , respectively, and both show relatively lower values of -7.2‰ and -2.3‰ at 10,760 cal yr BP.

4.2. Stage 2 (763–645 cm, 9800–5900 cal yr BP)

This stage can be subdivided into two sub-stages: sub-stage 2b (763–685 cm, 9800–7700 cal yr BP) and 2a (685–645 cm, 7700–5900 cal yr BP). In sub-stage 2b, quartz percentages are much higher than stage 3 but exhibit a decreasing trend and decrease from 73.6% to 57.6%; microcline percentages increase from 5.9% to 13.4% with a maximum of 22.1% at 8070 cal yr BP; albite and clinochlore percentages are also higher than stage 3 and they show averages of 14.4% and 2.9%, respectively; illite percentages average 3.7%. There is no signal of gypsum. Calcite percentages are much lower than stage 3 but exhibit an increasing trend and increase from 0 to 11.2% with their maximum of 24.2% at 7780 cal yr BP.

In sub-stage 2b, all of the chemical proxies exhibit low values but increasing trends from 9200 to 7700 cal yr BP. Ca and Mg concentrations, Mg/Ca ratios, and $\delta^{18}\text{O}$ and $\delta^{13}\text{C}$ values increase

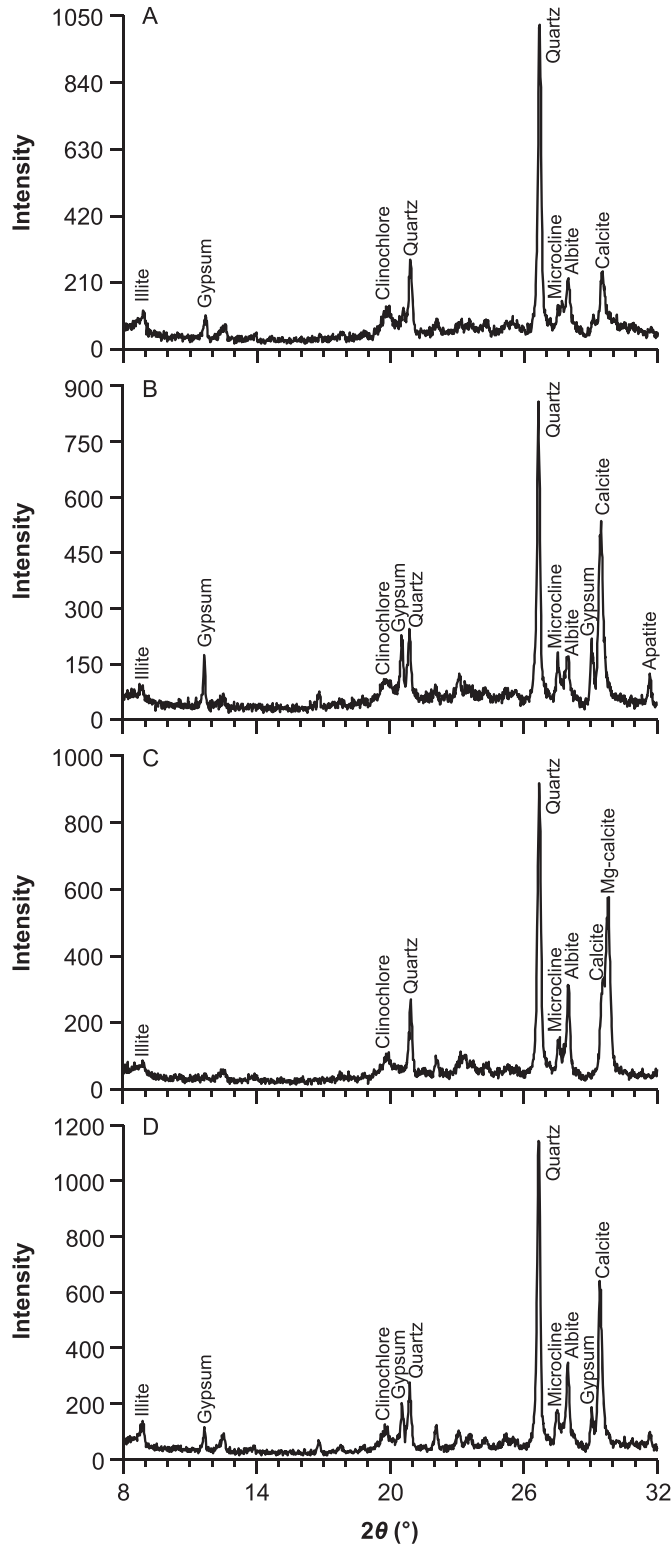


Fig. 2. X-ray diffractogram (XRD) ($8\text{--}32^\circ 2\theta$) for four representative bulk sediment samples at the depths of (A) 280 cm (2049 cal yr BP), (B) 608 cm (5291 cal yr BP), (C) 623 cm (5535 cal yr BP) and (D) 823 cm (11094 cal yr BP) from the upper 8.5 m of the DL04 core. Major peaks occur around 7.63 \AA ($11.62^\circ 2\theta$), 4.28 \AA ($20.72^\circ 2\theta$) and 3.07 \AA ($29.10^\circ 2\theta$) reflecting dominance of gypsum, and 3.03 \AA ($29.42^\circ 2\theta$) reflecting calcite.

gradually from 0.9%, 0.10%, 0.18, -8.3‰ and 0.9%, respectively, at 9200 cal yr BP, to 2.3%, 0.40%, 0.29, -5.9‰ and 2.9% at 7700 cal yr BP.

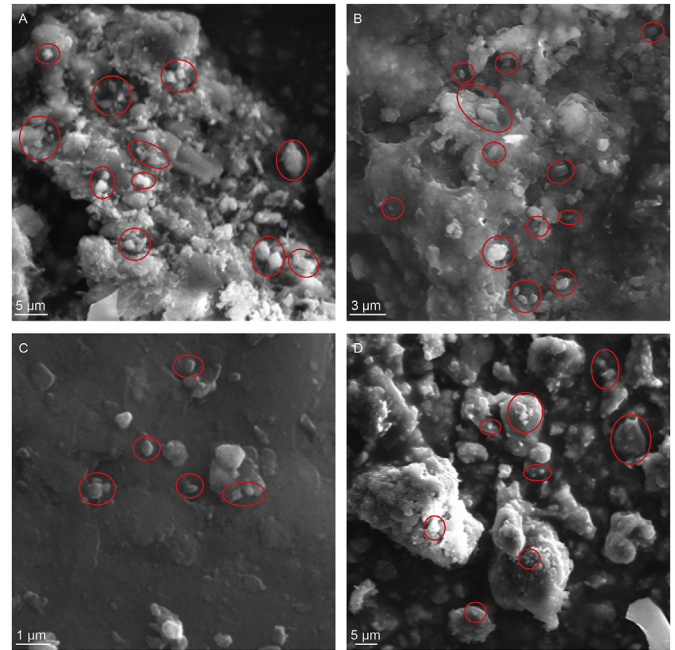


Fig. 3. Scanning electron microscope (SEM) images of the $<38\text{-}\mu\text{m}$ carbonates from four representative samples at the depths of (A) 217 cm (1500 cal yr BP), (B) 632 cm (5680 cal yr BP), (C) 698 cm (8300 cal yr BP) and (D) 802 cm (10800 cal yr BP) from the upper 8.5 m of the DL04 core. The carbonate crystals are marked by red circles. (A) and (B) are cited from Fan et al. (2016). (For interpretation of the references to colour in this figure legend, the reader is referred to the Web version of this article.)

In sub-stage 2a, quartz percentages reach the highest values of the last 11,500 cal yr and they show an average of 69.5%; microcline, albite and clinocllore percentages maintain high values with averages of 9.3%, 15.7% and 2.3%, respectively; illite percentages average 3.1%. There is no signal of gypsum and calcite.

4.3. Stage 1 (645–0 cm, 5900–0 cal yr BP)

This stage can be subdivided into two sub-stages: sub-stage 1b (645–573 cm, 5900–4850 cal yr BP) and 1a (573–0 cm, 4850–0 cal yr BP). In sub-stage 1b, quartz percentages decrease significantly and show an average of 49.5%; microcline, albite and clinocllore percentages decrease to averages of 7.8%, 10.5% and 1.8%, respectively; illite percentages increase slightly from 3.5% to 3.9%. Gypsum and calcite percentages increase significantly. Gypsum percentages increase from 0 to 4.8% with their maximum of 16.3% at 5290 cal yr BP; calcite percentages show an average of 23.0% with their maximum of 40.3% at 5680 cal yr BP, and Mg-calcite occurs from 5780 to 5430 cal yr BP.

In sub-stage 1b, Ca and Mg concentrations, Mg/Ca ratios and $\delta^{13}\text{C}$ values increase significantly. Ca and Mg concentrations and Mg/Ca ratios average 3.0%, 0.60% and 0.34, respectively. $\delta^{13}\text{C}$ values average 3.1‰. $\delta^{18}\text{O}$ values are relatively lower and they show an average of -5.0‰ .

In sub-stage 1a, quartz, microcline, albite, illite, and clinocllore percentages generally fluctuate between 43.7% and 74.3%, 3.7% and 19.8%, 8.6% and 23.1%, 1.4% and 12.4%, 0.3% and 5.3%, respectively. Gypsum percentages range from 0.9% to 8.9% from 4850 to 1240 cal yr BP, and there is no signal of gypsum during the last 1240 cal yr; calcite percentages range from 1.9% to 19.4% in this sub-stage.

Ca and Mg concentrations are relatively stable and high in sub-stage 1a, and they show averages of 2.7% and 0.51%, respectively. Mg/Ca ratios and $\delta^{18}\text{O}$ and $\delta^{13}\text{C}$ values exhibit slightly increasing

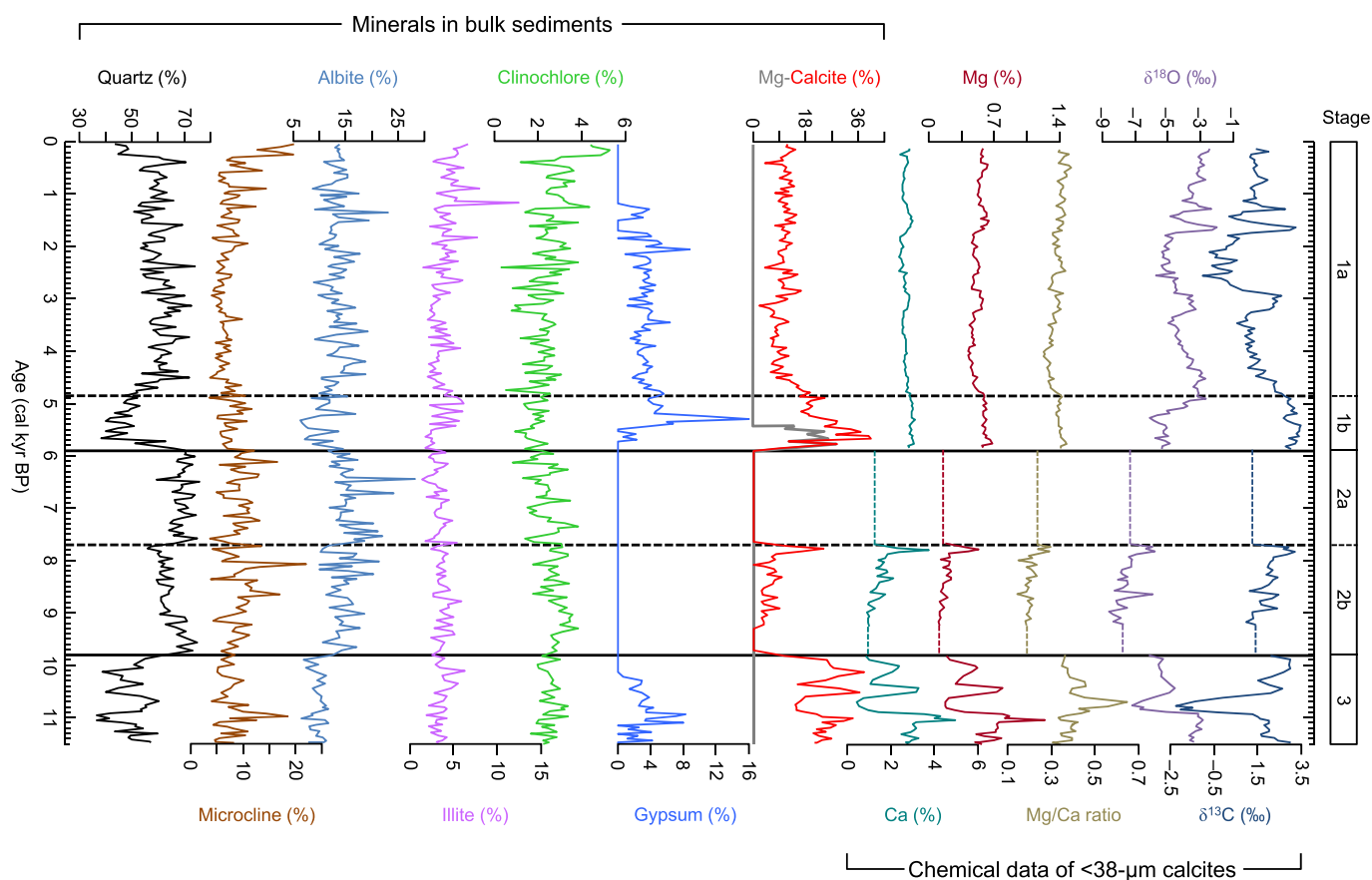


Fig. 4. Time series of quartz, microcline, albite, illite, clinocllore, gypsum and calcite percentages of bulk sediments, and Ca and Mg concentrations, Mg/Ca mole ratio and $\delta^{18}\text{O}$ and $\delta^{13}\text{C}$ values of $<38\text{-}\mu\text{m}$ calcites from the upper 8.5 m of the DL04 core spanning the last 11,500 cal yr. Gray curve indicates Mg-calcite percentage. Dashed vertical lines indicate no data. Horizontal solid and dashed lines bracket the stages and sub-stages characterizing the pattern of changes in these chemical data during the last 11,500 cal yr. The elemental and isotopic data of $<38\text{-}\mu\text{m}$ calcites from the upper 6.39 m of the DL04 core are cited from Fan et al. (2016).

trends in sub-stage 1a. Mg/Ca ratios range from 0.26 to 0.39. $\delta^{18}\text{O}$ and $\delta^{13}\text{C}$ values vary within the ranges of -5.7‰ to -2.0‰ and -1.1‰ to 3.2‰ , respectively, and both show peaks at 1570 cal yr BP.

The data of Ca and Mg concentrations, Mg/Ca ratios and $\delta^{18}\text{O}$ and $\delta^{13}\text{C}$ values of $<38\text{-}\mu\text{m}$ calcites during the last 6000 cal yr are cited from Fan et al. (2016).

5. Discussion

5.1. Interpretations of the multidisciplinary proxies

5.1.1. Minerals and elements

Minerals in lake sediments can be considered as either external to the lake (allogenic) or internal (endogenic and authigenic) (Lerman, 1978). In most lakes quartz, feldspar and some clay minerals, such as illite and clinocllore, are allogenic; while calcite, Mg-calcite and gypsum are common endogenic or authigenic minerals in brackish and moderately saline lakes (Eugster and Jones, 1979). Dali Lake is a brackish lake, and there is no outcrop of gypsum and carbonate rocks in the region (Li, 1993). Therefore calcites and gypsum in the lake sediments should be mainly from the lake internal. In order to remove biogenic calcites (such as ostracod shells which have relatively larger grain sizes, commonly $>63\text{ }\mu\text{m}$, e.g., Zhai et al., 2010), the $<38\text{-}\mu\text{m}$ calcites in the Dali Lake sediments were selected to do the geochemical analyses. Previous studies indicate that these fine calcites are mainly inorganic precipitated

(Fan et al., 2016). SEM images of the $<38\text{-}\mu\text{m}$ calcites from four representative samples from the DL04 core during the Holocene are granular, blocky, lenticular and prismatic idiomorphic, and generally $<10\text{ }\mu\text{m}$ in grain size (Fig. 3), denoting that these calcite crystals are endogenous origin and rapidly precipitated (Jiménez-López et al., 2004). Dali Lake is located in the semi-arid regions, the precipitation of calcites and gypsum in the lake should be closely related to the evaporative losses of lake water (Fan et al., 2016). The lake water is usually saturated with respect to CaCO_3 , when the evaporative losses of lake water overwhelm the water input (including runoff and rainfall) to the lake, CaCO_3 will be preferentially precipitated as calcite, resulting in progressively increased $\text{Mg}^{2+}/\text{Ca}^{2+}$ and $\text{SO}_4^{2-}/\text{Ca}^{2+}$ ratios of the lake water. When the $\text{Mg}^{2+}/\text{Ca}^{2+}$ ratio of lake water exceeds 2, Mg^{2+} will be incorporated into calcite to form Mg-calcite precipitation (Müller et al., 1972; Eugster and Jones, 1979; Ito and Forester, 2009). In addition, when the HCO_3^- in the lake water is largely consumed, the SO_4^{2-} will be combined with Ca^{2+} to form gypsum precipitation (Eugster and Jones, 1979). Therefore the precipitation of calcite, Mg-calcite and gypsum, and the Ca and Mg concentrations of endogenic calcites can be an indicator of hydrological balance of the lake. High percentages of these minerals and high values of these elements indicate less water input to the lake than evaporative losses, and vice versa. The opposite trends in the percentages, within analytical errors, between allogenic and endogenic/authigenic minerals, and the similar trends in the values between calcite percentages and elemental concentrations in the Dali Lake sediments during the

Holocene (Fig. 4) support that less water input to the lake than evaporative losses would result in less allogenic minerals transported to the lake while more endogenic/authigenic minerals precipitated in the lake and higher Ca and Mg concentrations, and vice versa.

5.1.2. Stable isotopes

The $\delta^{18}\text{O}$ value of lacustrine endogenic calcite is a function of the $\delta^{18}\text{O}$ value and temperature of lake water. An increase of 1‰ in the calcite $\delta^{18}\text{O}$ value can be caused either by an increase of 1‰ in the water $\delta^{18}\text{O}$ value or by a decrease of 4–5 °C in the water temperature, or by a combination of both, in the equilibrium of oxygen isotopic fractionation (Kim and O'Neil, 1997). The endogenic calcites from the DL04 core exhibit a large variation of up to 6.6‰ in the $\delta^{18}\text{O}$ values during the Holocene (Fig. 4), implying that the calcite $\delta^{18}\text{O}$ mainly depended on the water $\delta^{18}\text{O}$. For closed lakes in the semi-arid regions, the water $\delta^{18}\text{O}$ values are primarily controlled by the balance between evaporative losses of lake water and the water input to the lake, provided that the source water in the region remains essentially unchanged (Lister et al., 1991; Ricketts and Johnson, 1996). When the evaporation intensifies, more H_2^{16}O would escape from lake water to the atmosphere, leading to the enrichment in ^{18}O of lake water and thus increases in the $\delta^{18}\text{O}$ values of endogenic calcites, and vice versa (Talbot, 1990). It is noticeable that changes in water or moisture sources can regulate the effect of hydrological balance on the $\delta^{18}\text{O}$ values of lake water, especially in lakes that usually collect various sources of water from rainfalls, snow/ice melt water and/or groundwater from large catchments (Ricketts et al., 2001) or receive different sources of moisture from different regions (Maher, 2008; Tan, 2014; Qiang et al., 2017). In this case, the $\delta^{18}\text{O}$ values of lake water would be also closely related to that of source water or moisture.

The $\delta^{13}\text{C}$ value of lacustrine endogenic calcite is mainly controlled by the $\delta^{13}\text{C}$ value of the lake's dissolved inorganic carbon pool ($\delta^{13}\text{C}_{\text{DIC}}$) that is affected by various factors such as the $\delta^{13}\text{C}$ value of the inflowing riverine DIC, primary productivity of the aquatic phytoplankton, burial and degradation of the sedimentary organic matter and the isotopic exchange between the lake's DIC pool and atmospheric CO_2 (Talbot, 1990; Talbot and Johannessen, 1992; Talbot and Lærdal, 2000; Leng and Marshall, 2004). Increases in the water input from the inflowing rivers would decrease the $\delta^{13}\text{C}$ value of the lake's DIC pool and thus of the endogenic calcites in the Dali Lake sediments because the $\delta^{13}\text{C}$ values of the inflowing riverine DIC are much lower than that of the lake's DIC pool (Fan et al., 2016). For hydrologically closed, oligotrophic lakes such as Dali Lake, the ^{13}C exchange between the lake's DIC pool and atmospheric CO_2 could be considered as an important factor controlling the variations in the $\delta^{13}\text{C}_{\text{DIC}}$ values of the lake. The degree of the ^{13}C exchange depends on the residence time and alkalinity of the lake water. Under a condition of intensified evaporation in the region, prolonged water residence time and elevated alkalinity would enhance the ^{13}C exchange, resulting in a ^{13}C -enriched lake's DIC pool (Talbot, 1990; Li and Ku, 1997; Leng and Marshall, 2004). The $\delta^{13}\text{C}$ and $\delta^{18}\text{O}$ values of endogenic calcites from the DL04 core during each stage/sub-stage exhibit a close covariation (Fig. 5), suggesting that the hydrological balance of lake water (water input versus evaporative losses) was the common factor that influenced the concentrations of both ^{18}O in the lake water and ^{13}C in the lake's DIC pool (Talbot, 1990), e.g., positive balance of the lake water would result in more negative $\delta^{13}\text{C}$ and $\delta^{18}\text{O}$ values of endogenic calcites, and vice versa. However, for the whole Holocene there is no significant relationship between $\delta^{13}\text{C}$ and $\delta^{18}\text{O}$ values of endogenic calcites ($r = 0.01$), which could be ascribed to the significantly low $\delta^{18}\text{O}$ values from 9200 to 7700 cal yr BP (Figs. 4 and 5). The

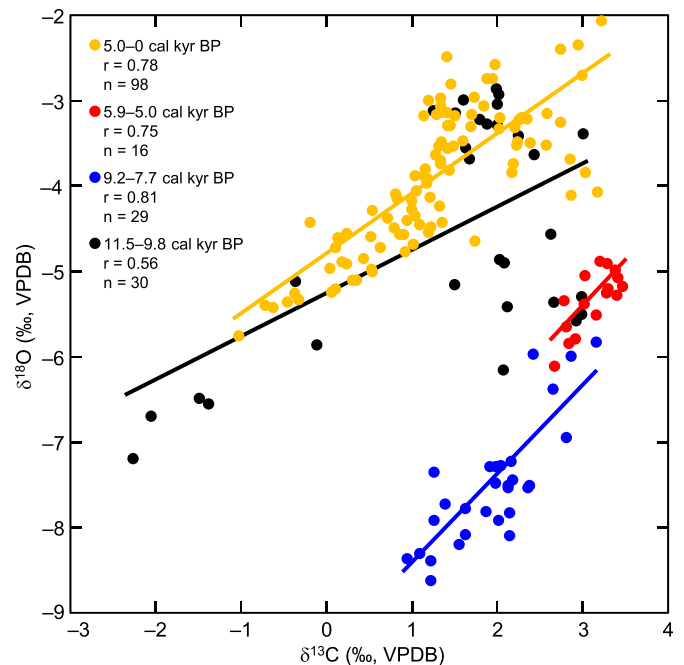


Fig. 5. Relationship between $\delta^{18}\text{O}$ and $\delta^{13}\text{C}$ values of $<38\text{-}\mu\text{m}$ calcites from the DL04 core for the last 11,500 cal yr. The data from the upper 6.39 m of the DL04 core are cited from Fan et al. (2016).

significantly low $\delta^{18}\text{O}$ values may imply the different sources of water or moisture supplied for the lake.

5.2. Holocene hydrological variations in the Dali Lake basin

The minerals in bulk samples, and elements and stable isotopes of endogenic calcites of the Dali Lake sediments from the DL04 core reveal a detailed history of changes in the hydrological variations in the lake basin during the Holocene (Fig. 4).

From 11,500 to 9800 cal yr BP, the percentages of the dominant allogenic minerals (quartz, microcline and albite) are relatively low while endogenic/authigenic minerals (gypsum and calcite) are high (Fig. 4), and Ca and Mg concentrations and $\delta^{18}\text{O}$ and $\delta^{13}\text{C}$ values are high (Fig. 4), indicating that the evaporative losses of lake water generally overwhelmed the water input to the lake during the 1700 cal yrs of this period. There was no Mg-calcite occurring in this period, which may be related to the thermodynamic instability of the Mg-calcite. In addition, significantly decreased values of the elements and stable isotopes at the interval of 10,850–10,550 cal yr BP (Fig. 4) may have resulted from a brief increased input of fresh water with low $\delta^{18}\text{O}$ and $\delta^{13}\text{C}_{\text{DIC}}$ values to the lake. The significantly low $\delta^{18}\text{O}$ values (with an average of -6.6‰) from 10,850 to 10,550 cal yr BP may have corresponded to the lowest $\delta^{18}\text{O}$ values (with an average of -15.3‰) of the inflowing water from Gongger River during the spring floods, when large amount of snow/ice melt water supplied for the river (Fan et al., 2016). At present the lake water has an average $\delta^{18}\text{O}$ value of -2.1‰ in June, about 8.7‰ higher than the inflowing water from Gongger River (-10.8‰) in the rainy season (Fan et al., 2016). If such a fractionation factor between inflowing water and lake water did not fluctuate largely during the late spring and summer, it may explain the difference of $\delta^{18}\text{O}$ values between endogenic calcites and melt water from 10,850 to 10,550 cal yr BP. In addition, previous studies on the sedimentary organic matter from the same lake indicate that terrestrial vegetation in the lake catchment was dominated by C_3 plants, which have much lower $\delta^{13}\text{C}$ values (-27.1‰) than the

lake's DIC pool (-0.3‰) (Fan et al., 2016, 2017). During the interval from 10,850 to 10,550 cal yr BP, organic matter from terrestrial plants input to the lake significantly increased (Fan et al., 2017); and the concomitant input of dissolved carbon released from degradation of these organic matter to the lake may have been responsible for significant decreases in the $\delta^{13}\text{C}$ values of the lake's DIC pool and thus the endogenic calcites. However, the Mg/Ca ratios show exceptionally high values during this interval (Fig. 4). The use of acetic acid should minimize the extraction of Ca from feldspar and Mg from clay minerals and organic matter (Haskell et al., 1996; Fan et al., 2016), but the dissolution of even a small amount of these materials will largely affect the values of Mg/Ca ratios of endogenic calcites. Regarding the uncertainties of Mg/Ca ratios from different sources of Ca and Mg leached by the acid (Haskell et al., 1996), only Ca and Mg concentrations are largely discussed in this study.

During the period from 9800 to 7700 cal yr BP, quartz, microcline and albite percentages increase significantly while gypsum and calcite percentages, and Ca and Mg concentrations and $\delta^{18}\text{O}$ and $\delta^{13}\text{C}$ values decrease significantly relative to the preceding period, suggesting that the water input to the lake increased significantly and exceeded the evaporative losses of lake water. In addition, there is an overall decreasing trend in quartz percentages but increasing trends in calcite percentages and elements and stable isotopes within this period, which imply that the inflowing water exhibited a decreasing trend in the 2100 yrs of this period. It is noticeable that the $\delta^{18}\text{O}$ values from 9800 to 7700 cal yr BP (range from -8.3‰ to -5.9‰) are much lower than the latter period from 5900 to 4850 cal yr BP (with an average of -4.1‰), while the $\delta^{13}\text{C}$ values during this period (with an average of 1.9‰) are higher than the latter period (with an average of 1.5‰) (Fig. 4). The $\delta^{18}\text{O}$ values from 9800 to 7700 cal yr BP are close to those from 10,850 to 10,550 cal yr BP (Fig. 4), implying that the source water of the lake may have been originated from the snow/ice melt water during this period. In addition, when the inflowing water increased, large amount of nutrient input to the lake increased, resulting in progressive increases in primary productivity of the lake (Fan et al., 2017). Aquatic phytoplankton preferentially assimilate dissolved ^{12}C in the lake water (Talbot and Johannessen, 1992; Talbot and Lærdal, 2000), leading to ^{13}C enriched DIC pool of the lake. Therefore the relatively high $\delta^{13}\text{C}$ values from 9800 to 7700 cal yr BP may have been ascribed to the high primary productivity of the lake (Fan et al., 2017).

The period between 7700 and 5900 cal yr BP is characterized by the highest quartz percentages but lowest gypsum and calcite percentages through the entire Holocene, and microcline and albite percentages maintain high values. These data imply that the water input to the lake further increased and the lake level reached the highest of the entire Holocene.

Compared with the preceding period of 9800–5900 cal yr BP, the period of 5900–4850 cal yr BP is characterized by significantly decreased quartz, microcline and albite percentages but significantly increased gypsum and calcite percentages and elements and stable isotopes, in addition Mg-calcite occurred during the first half of the period from 5900 to 4850 cal yr BP. These data suggest that the inflowing water dramatically decreased and was much less than the evaporative losses of lake water, resulting in significantly decreased lake level from 5900 to 4850 cal yr BP. The relatively low $\delta^{18}\text{O}$ values in this period (Fig. 4) may have been caused by the rapid precipitation of endogenic calcites or the inheritance of the $\delta^{18}\text{O}$ values of lake water (Fan et al., 2016).

Since 4850 cal yr BP, quartz and albite percentages increase to a higher level relative to the preceding period of 5900–4850 cal yr BP, but are much lower than the period of 9800–5900 cal yr BP. These data indicate that the net losses of lake water were much less from 4850 to 0 cal yr BP than from 5900 to 4850 cal yr BP, although

the inflowing water to the lake maintained a low level during the last 4850 cal yrs. Such inferences could be supported by the overall high calcite percentages and high values of Ca and Mg concentrations and $\delta^{18}\text{O}$ and $\delta^{13}\text{C}$ in the last 4850 cal yrs of the Holocene. In addition, the absence of gypsum during the last 1240 cal yrs might be ascribed to the high $\text{HCO}_3^-/\text{SO}_4^{2-}$ ratios of the lake water due to the degradation of sedimentary organic matter (Fan et al., 2017).

5.3. Possible causes of Holocene hydrological variations

The evidences from mineralogy and carbonate geochemistry of the Dali Lake sediments indicate that the inflowing water to the lake was low or the evaporative losses of lake water was high from 11,500 to 9800 cal yr BP (Fig. 6). At which time regional precipitation maintained a very low level as suggested by the low tree percentages from the same lake (Wen et al., 2017) and from a nearby lake, Daihai Lake in the EASM margin (Xiao et al., 2004) (Figs. 1 and 6). Meanwhile, summer insolation in the NH gradually increased (Laskar et al., 2004) (Fig. 6), which may have resulted in increased temperature in the EASM margin. Therefore we suggest that the dry climate and high temperature in the EASM margin have caused the negative balance of the lake water (inflowing water less than evaporative losses) from 11,500 to 9800 cal yr BP. However, the $\delta^{18}\text{O}$ values of stalagmites from Lianhua Cave close to the Daihai Lake are relatively low during this period, and much lower than late Holocene (Dong et al., 2015) (Figs. 1 and 6). Therefore we speculate that changes in stalagmite $\delta^{18}\text{O}$ values may have been, to some extent, resulted from changes in the $\delta^{18}\text{O}$ values of moisture sources. During the early Holocene, the distance between Lianhua Cave and monsoonal source area should be longer than present due to the remnant ice sheets in Northern Hemisphere (NH) (Dyke, 2004; Carlson et al., 2008; Parducci et al., 2012) and the resultant lower sea levels (Li et al., 2014), and the longer distance for the transportation of moisture from monsoonal source area to the Lianhua Cave area during the early Holocene would result in lower $\delta^{18}\text{O}$ values of the moisture and thus of the stalagmites (Tan, 2014). Furthermore, if the stalagmite $\delta^{18}\text{O}$ values from Lianhua Cave were controlled by the rainfall-amount effect, it is unlikely that there is only a difference of 1‰ – 2‰ in the $\delta^{18}\text{O}$ values of stalagmites between Dongge Cave in the low latitude (Wang et al., 2005; Dykoski et al., 2005) and Lianhua Cave in the middle latitude (Dong et al., 2015) during the early Holocene (Fig. 1). These data further support that the $\delta^{18}\text{O}$ values of stalagmites from Lianhua Cave during the early Holocene may reflect the $\delta^{18}\text{O}$ values of moisture.

There were large amount of inflowing water supplying for Dali Lake from 9800 to 7700 cal yr BP, however, regional precipitation remained at a low level during this period (Fig. 6). It is noticeable that NH summer insolation reached a maximum (7% greater than the present value) at ca. 10,000 cal yr BP (Laskar et al., 2004) (Fig. 6). We thus infer that the inflowing water may have mainly been originated from the snow/ice melt water from the surrounding mountains in response to the persistent warming in the EASM margin induced by the high NH summer insolation during the early Holocene. Modern hydrological observations show that the major inflow to Dali Lake, the Gongger River, rises in the southern terminal part of the Great Hinggan Mountains, generally discharges melt water during spring floods as large as during summer floods (Li, 1993). These observations support the inference that snow and ice melt water inflowing to the lake played an important role in the hydrological balance of the lake during this period. In addition, the significantly low $\delta^{18}\text{O}$ values of endogenic calcites from the Dali Lake sediments from 9800 to 7700 cal yr BP (Figs. 4 and 6) correspond to the lowest $\delta^{18}\text{O}$ values of inflowing water from the Gongger River during the spring floods (Fan et al., 2016). These data further support the above inference (see discussion 5.2.). The

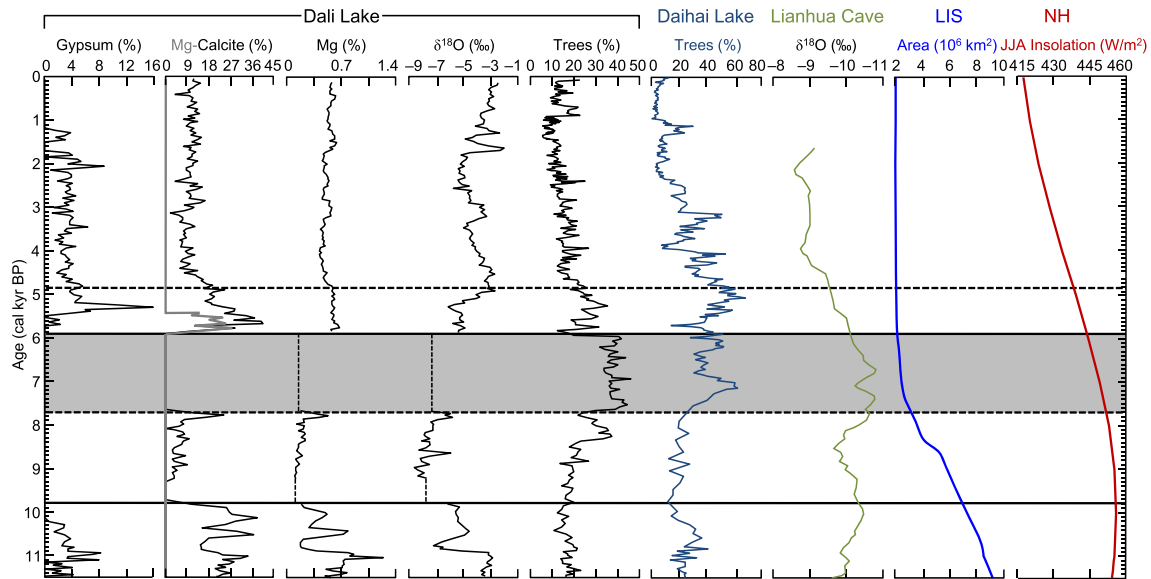


Fig. 6. Correlation of gypsum and calcite percentages in bulk samples, Mg concentration and $\delta^{18}\text{O}$ value of $<38\text{-}\mu\text{m}$ calcites of the Dali Lake sediments from the DL04 core spanning the last 11,500 cal yr with tree percentages from the same lake (Wen et al., 2017) and from Daihai Lake (Xiao et al., 2004), and with 5-point averaged $\delta^{18}\text{O}$ value of stalagmite from Lianhua Cave (Dong et al., 2015), Laurentide Ice Sheet (LIS) area (Dyke, 2004) and Northern Hemisphere (NH, 65°N) summer (June, July and August, JJA) insolation (Laskar et al., 2004). Gray curve indicates Mg-calcite percentage. Dashed vertical lines indicate no data. Horizontal solid and dashed lines indicate the stages and sub-stages characterizing the pattern of changes in the hydrology and climate in the Dali Lake region during the last 11,500 cal yr. Shaded bar indicates the highest water level of Dali Lake through the entire Holocene. The data of Mg concentration and $\delta^{18}\text{O}$ value of $<38\text{-}\mu\text{m}$ calcites from the upper 6.39 m of the DL04 core are cited from Fan et al. (2016).

decreasing trend of inflowing snow/ice melt water in this period may have responded to the slight decreases in the NH summer insolation from 10,000 to 8000 cal yr BP (Fig. 6). By the way, the oxygen isotopic composition of stalagmites growing from drip water in caves could record the average of $\delta^{18}\text{O}$ values of multi-year moisture or precipitation (Duan et al., 2016). The $\delta^{18}\text{O}$ values of moisture reflected by the stalagmites from Lianhua Cave generally range from -10.5‰ to -9.6‰ during the early Holocene (Dong et al., 2015) (Fig. 6). These moisture could not be responsible for the significantly low $\delta^{18}\text{O}$ values (-8.3‰ to -5.9‰) of endogenic calcites from Dali Lake from 9200 to 7700 cal yr BP as well as 10,850–10,550 cal yr BP (Fig. 6), under the condition of a fractionation factor of 8.7‰ for oxygen isotopes between the inflowing water and the lake water (see discussion 5.2.). Therefore the high water level of Dali Lake at the above two intervals could not be caused by significantly increased regional precipitation.

From 7700 to 5900 cal yr BP, the inflowing water to Dali Lake significantly increased, at the same time regional precipitation increased to the highest level of the entire Holocene (Fig. 6). These data imply that regional precipitation must have made great contributions to the hydrological balance of the lake during this period. Dali Lake is located in the modern northern margin of the EASM (Fig. 1). Meteorological observations indicate that most of the annual precipitation in the region falls in summer when the EASM penetrates into its modern northern limit (Li, 1993). These data imply that past changes in precipitation in the Dali Lake region were closely related to variations in the EASM intensity. The increase in precipitation would be indicative of the intensification of the EASM. The EASM circulation is driven by seasonal changes in the thermal contrast between the tropical Pacific and the Asian continent (An, 2000). During the early Holocene before 7700 cal yr BP, the northward migration of the monsoonal rain belt may have been hampered by the NH remnant ice sheets (Dyke, 2004) (Fig. 6) as well as the relatively lower global sea level (Peltier and Fairbanks, 2006) despite increases in the NH summer insolation (Laskar et al., 2004) (Fig. 6) and in sea surface temperatures (SST) of

the western tropical Pacific (Stott et al., 2004). At 8000–6000 cal yr BP, ice sheets in the NH high-latitudes retreated to the present extent (Dyke, 2004) (Fig. 6), while the global sea level rose to its current configuration (Peltier and Fairbanks, 2006). Such changes in the boundary conditions could help enhance the thermal contrast between the tropical Pacific and the Asian continent, and shorten the distance from the Asian interior to the source areas of the monsoonal moisture, thereby leading to further northerly penetration of the monsoon rain belt beyond its modern northern limit, and significant increases in precipitation in the present monsoon margin. In addition, significant increases in regional precipitation could have further decreased the $\delta^{18}\text{O}$ values of stalagmites from Lianhua Cave during this period (Dong et al., 2015) (Fig. 6).

The inflowing water to Dali Lake dramatically decreased and the evaporation significantly intensified at ca. 5900 cal yr BP, which could be related to the significant decreases in the monsoonal precipitation (Fig. 6). The significantly weakening of the monsoonal precipitation at ca. 5900 cal yr BP matches very well with the most prominent ice-rafted debris in the North Atlantic (Bond et al., 2001), and corresponds in time to the decreases in SST of the western tropical Pacific (Stott et al., 2004), highlighting the important influence of the cooling over northern high latitudes and western tropical Pacific on regulating the EASM circulation on millennial timescales (Li et al., 2018).

After 5900–4850 cal yr BP, the inflowing water to the lake maintained a low level, which should be caused by the decreases in the monsoonal precipitation (Fig. 6). The gradual decreases in the monsoonal precipitation may have been triggered by gradually decreased SST of the western tropical Pacific (Stott et al., 2004) and the NH summer insolation (Laskar et al., 2004) (Fig. 6).

6. Conclusions

This study presents $\sim 50\text{-yr}$ resolution, well-dated records of minerals in bulk samples and elements and stable isotopes of $<38\text{-}\mu\text{m}$

μm calcites (endogenic calcites) from a sediment core from Dali Lake, in order to detect the patterns and mechanisms of Holocene hydrological variations in the modern northern margin of the EASM. Increases in the percentages of allogenic minerals (quartz, microcline and albite) and decreases in the percentages of endogenic/autigenic minerals (calcite, Mg-calcite and gypsum), together with decreases in the values of Ca and Mg concentrations and $\delta^{18}\text{O}$ and $\delta^{13}\text{C}$ of endogenic calcites indicate an excess of water input to the lake over evaporative losses, and vice versa. These data suggest that the hydrological balance of Dali Lake was controlled by strong evaporation before 9800 cal yr BP, and then supplied by significantly enhanced inflowing water between 9800 and 5900 cal yr BP. From 5900 to 4850 cal yr BP, the water input to the lake significantly decreased. Since 4850 cal yr BP, the inflowing water maintained a low level. In addition, there were significant differences in the mineralogy and carbonate geochemistry of the Dali Lake sediments between the periods of 9800–7700 and 7700–5900 cal yr BP. The distinct characteristics of high water level of Dali Lake between these two periods may imply that the lake was mainly fed by snow/ice melt water from 9800 to 7700 cal yr BP and then by regional precipitation from 7700 to 5900 cal yr BP, which was further supported by the pollen records from the same sediment core. These results indicate that Holocene hydrological variations in the Dali Lake basin in the EASM margin were closely related to changes in regional temperature and precipitation which were ultimately controlled by changes in the NH summer insolation, northern high latitude ice sheets, global sea level and physicochemical conditions of the North Atlantic and western tropical Pacific on orbital and millennial timescales.

Acknowledgements

The authors are grateful to Prof. Dr. Min-Te Chen and Sangheon Yi and two anonymous reviewers for the improvement of the early version of this manuscript. This study is supported by the National Key Research and Development Program of China (2017YFA0603400), National Natural Science Foundation of China (41702179, 41130101 and 41672166) and China Postdoctoral Science Foundation (2017M610111).

Appendix A. Supplementary data

Supplementary data related to this article can be found at <https://doi.org/10.1016/j.quaint.2018.03.019>.

References

- An, Z.S., 2000. The history and variability of the East Asian paleomonsoon climate. *Quat. Sci. Rev.* 19, 171–187.
- An, Z.S., Colman, S.M., Zhou, W.J., Li, X.Q., Brown, E.T., Jull, A.J.T., Cai, Y.J., Huang, Y.S., Lu, X.F., Chang, H., Song, Y.G., Sun, Y.B., Xu, H., Liu, W.G., Jin, Z.D., Liu, X.D., Cheng, P., Liu, Y., Ai, L., Li, X.Z., Liu, X.J., Yan, L.B., Shi, Z.G., Wang, X.L., Wu, F., Qiang, X.K., Dong, J.B., Lu, F.Y., Xu, X.W., 2012. Interplay between the westerlies and Asian monsoon recorded in lake Qinghai sediments since 32 ka. *Sci. Rep.* 2, 619. <https://doi.org/10.1038/srep00619>.
- An, Z.S., Porter, S.C., Kutzbach, J.E., Wu, X.H., Wang, S.M., Liu, X.D., Li, X.Q., Zhou, W.J., 2000. Asynchronous Holocene optimum of the east Asian monsoon. *Quat. Sci. Rev.* 19, 743–762.
- Bond, G., Kromer, B., Beer, J., Muscheler, R., Evans, M.N., Showers, W., Hoffmann, S., Lotti-Bond, R., Hajdas, I., Bonani, G., 2001. Persistent solar influence in north Atlantic climate during the Holocene. *Science* 294, 2130–2136.
- Carlson, A.E., Legrande, A.N., Oppo, D.W., Came, R.E., Schmidt, G.A., Anslow, F.S., Licciardi, J.M., Obbink, E.A., 2008. Rapid early Holocene deglaciation of the Laurentide ice sheet. *Nat. Geosci.* 1, 620–624.
- Chen, F.H., Xu, Q.H., Chen, J.H., Birks, H.J.B., Liu, J.B., Zhang, S.R., Jin, L.Y., An, C.B., Telford, R.J., Cao, X.Y., Wang, Z.L., Zhang, X.J., Selvaraj, K., Lu, H.Y., Li, Y.C., Zheng, Z., Wang, H.P., Zhou, A.F., Dong, G.H., Zhang, J.W., Huang, X.Z., Bloemendal, J., Rao, Z.G., 2015. East Asian summer monsoon precipitation variability since the last deglaciation. *Sci. Rep.* 5, 11186. <https://doi.org/10.1038/srep11186>.
- Chen, F.H., Yu, Z.C., Yang, M.L., Ito, E., Wang, S.M., Madsen, D.B., Huang, X.Z., Zhao, Y., Sato, T., Birks, H.J.B., Boomer, I., Chen, J.H., An, C.B., Wünnemann, B., 2008. Holocene moisture evolution in arid central Asia and its out-of-phase relationship with Asian monsoon history. *Quat. Sci. Rev.* 27, 351–364.
- Cheng, H., Edwards, R.L., Sinha, A., Spötl, C., Yi, L., Chen, S.T., Kelly, M., Kathayat, G., Wang, X.F., Li, X.L., Kong, X.G., Wang, Y.J., Ning, Y.F., Zhang, H.W., 2016. The Asian monsoon over the past 640,000 years and ice age terminations. *Nature* 534, 640–646.
- Dong, J.G., Shen, C.-C., Kong, X.G., Wang, H.-C., Jiang, X.Y., 2015. Reconciliation of hydroclimate sequences from the Chinese loess plateau and low-latitude East Asian summer monsoon regions over the past 14,500 years. *Palaeogeography, Palaeoclimatology, Palaeoecology* 435, 127–135.
- Duan, W.H., Ruan, J.Y., Luo, W.J., Li, T.Y., Tian, L.J., Zeng, G.N., Zhang, D.Z., Bai, Y.J., Li, J.L., Tao, T., Zhang, P.Z., Baker, A., Tan, M., 2016. The transfer of seasonal isotopic variability between precipitation and drip water at eight caves in the monsoon regions of China. *Geochim. Cosmochim. Acta* 183, 250–266.
- Dyke, A.S., 2004. An outline of North American deglaciation with emphasis on central and northern Canada. *Quat. Glaciat. – Extent Chronology* 2, 373–424.
- Dykoski, C.A., Edwards, R.L., Cheng, H., Yuan, D.X., Cai, Y.J., Zhang, M.L., Lin, Y.S., Qing, J.M., An, Z.S., Revenaugh, J., 2005. A high-resolution, absolute-dated Holocene and deglacial Asian monsoon record from Dongge Cave, China. *Earth Planet. Sci. Lett.* 233, 71–86.
- Eugster, H.P., Jones, B.F., 1979. Behavior of major solutes during closed-basin brine evolution. *Am. J. Sci.* 279, 609–631.
- Fan, J.W., Xiao, J.L., Wen, R.L., Zhang, S.R., Wang, X., Cui, L.L., Li, H., Xue, D.S., Yamagata, H., 2016. Droughts in the East Asian summer monsoon margin during the last 6 kyr: link to the North Atlantic cooling events. *Quat. Sci. Rev.* 151, 88–99.
- Fan, J.W., Xiao, J.L., Wen, R.L., Zhang, S.R., Wang, X., Cui, L.L., Yamagata, H., 2017. Carbon and nitrogen signatures of sedimentary organic matter from Dali Lake in Inner Mongolia: implications for Holocene hydrological and ecological variations in the East Asian summer monsoon margin. *Quat. Int.* 452, 65–78.
- Goldsmith, Y., Broecker, W.S., Xu, H., Polissar, P.J., deMenocal, P.B., Porat, N., Lan, J.H., Cheng, P., Zhou, W.J., An, Z.S., 2017. Northward extent of East Asian monsoon covaries with intensity on orbital and millennial timescales. *Proc. Natl. Acad. Sci. U. S. A.* 114, 1817–1821.
- Haskell, B.J., Engstrom, D.R., Fritz, S.C., 1996. Late quaternary paleohydrology in the north American great plains inferred from the geochemistry of endogenic carbonate and fossil ostracodes from Devils Lake, north Dakota, USA. *Palaeogeography, Palaeoclimatology, Palaeoecology* 124, 179–193.
- Ito, E., Forester, R.M., 2009. Changes in continental ostracode shell chemistry: uncertainty of cause. *Hydrobiologia* 620, 1–15.
- Jiménez-López, C., Romanek, C.S., Huertas, F.J., Ohmoto, H., Caballero, E., 2004. Oxygen isotope fractionation in synthetic magnesian calcite. *Geochim. Cosmochim. Acta* 68, 3367–3377.
- Kim, S.T., O'Neil, J.R., 1997. Equilibrium and nonequilibrium oxygen isotope effects in synthetic carbonates. *Geochim. Cosmochim. Acta* 61, 3461–3475.
- Laskar, J., Robutel, P., Joutel, F., Gastineau, M., Correia, A.C.M., Levrard, B., 2004. A long term numerical solution for the insolation quantities of the Earth. *Astron. Astrophys.* 428, 261–285.
- Leng, M.J., Marshall, J.D., 2004. Palaeoclimate interpretation of stable isotope data from lake sediment archives. *Quat. Sci. Rev.* 23, 811–831.
- Lerman, A., 1978. *Lakes: Chemistry, Geology, Physics*. Springer, 363 pp.
- Li, G.X., Li, P., Liu, Y., Qiao, L.L., Ma, Y.Y., Xu, J.S., Yang, Z.G., 2014. Sedimentary system response to the global sea level change in the East China Seas since the last glacial maximum. *Earth Sci. Rev.* 139, 390–405.
- Li, H.C., Bar-Matthews, M., Chang, Y.P., Ayalon, A., Yuan, D.X., Zhang, M.L., Lone, M.A., 2017a. High-resolution $\delta^{18}\text{O}$ and $\delta^{13}\text{C}$ records during the past 65 ka from Fengyu Cave in Guilin: variation of monsoonal climates in south China. *Quat. Int.* 441, 117–128.
- Li, H.C., Ku, T.L., 1997. $\delta^{13}\text{C}$ – $\delta^{18}\text{O}$ covariance as a paleohydrological indicator for closed-basin lakes. *Palaeogeogr. Palaeoclimatol. Palaeoecol.* 133, 69–80.
- Li, N.N., Chambers, F.M., Yang, J.X., Jie, D.M., Liu, L.D., Liu, H.Y., Gao, G.Z., Gao, Z., Li, D.H., Shi, J.C., Feng, Y.Y., Qiao, Z.H., 2017b. Records of East Asian monsoon activities in Northeastern China since 15.6 ka, based on grain size analysis of peaty sediments in the Changbai Mountains. *Quat. Int.* 447, 158–169.
- Li, Q., Li, G.X., Chen, M.-T., Cheng, H., Xu, J.S., Ding, D., Ma, Y.Y., Qiao, L.L., Zhang, Q., Zhang, Y., Wang, H.Y., An, Z.Z., Min, J.X., Wang, L.Y., 2018. East Asian summer monsoon variations during the last deglaciation, recorded from a stalagmite at Linyi, northern China. *Quat. Int.* 464, 327–335.
- Li, Z.G., 1993. *Annals of Hexigten Banner*. People's Press of Inner Mongolia, Hohhot, 1144 pp (in Chinese).
- Lister, G.S., Kelts, K., Chen, K.Z., Yu, J.Q., Niessen, F., 1991. Lake Qinghai, China: closed-basin lake levels and the oxygen isotope record for ostracoda since the latest Pleistocene. *Palaeogeogr. Palaeoclimatol. Palaeoecol.* 84, 141–162.
- Liu, D.B., Wang, Y.J., Cheng, H., Edwards, R.L., Kong, X.G., 2017. Remote vs. local control on the Preboreal Asian hydroclimate and soil processes recorded by an annually-laminated stalagmite from Daoguan Cave, southern China. *Quat. Int.* 452, 79–90.
- Maher, B.A., 2008. Holocene variability of the East Asian summer monsoon from Chinese cave records: a re-assessment. *Holocene* 18, 861–866.
- Müller, G., Irion, G., Förstner, U., 1972. Formation and diagenesis of inorganic Ca-Mg carbonates in the lacustrine environment. *Naturwissenschaften* 59, 158–164.
- Parducci, L., Jørgensen, T., Tollefsrud, M.M., Elverland, E., Alm, T., Fontana, S.L., Bennett, K.D., Haile, J., Matetovici, I., Suyama, Y., Edwards, M.E., Andersen, K.,

- Rasmussen, M., Boessenkool, S., Coissac, E., Brochmann, C., Taberlet, P., Houmark-Nielsen, M., Larsen, N.K., Orlando, L., Gilbert, M.T.P., Kjær, K.H., Alsos, I.G., Willerslev, E., 2012. Glacial survival of boreal trees in northern scandinavia. *Science* 335, 1083–1086.
- Peltier, W.R., Fairbanks, R.G., 2006. Global glacial ice volume and Last Glacial Maximum duration from an extended Barbados sea level record. *Quat. Sci. Rev.* 25, 3322–3337.
- Porter, S.C., Zhou, W.J., 2006. Synchronism of Holocene East Asian monsoon variations and North Atlantic drift-ice tracers. *Quat. Res.* 65, 443–449.
- Qiang, M.R., Song, L., Jin, Y.X., Li, Y., Liu, L., Zhang, J.W., Zhao, Y., Chen, F.H., 2017. A 16-ka oxygen-isotope record from Genggahai Lake on the northeastern Qinghai-Tibetan Plateau: hydroclimatic evolution and changes in atmospheric circulation. *Quat. Sci. Rev.* 162, 72–87.
- Ricketts, R.D., Johnson, T.C., 1996. Climate change in the Turkana basin as deduced from a 4000 year long $\delta^{18}\text{O}$ record. *Earth Planet. Sci. Lett.* 142, 7–17.
- Ricketts, R.D., Johnson, T.C., Brown, E.T., Rasmussen, K.A., Romanovsky, V.V., 2001. The Holocene paleolimnology of Lake Issyk-Kul, Kyrgyzstan: trace element and stable isotope composition of ostracodes. *Palaeogeogr. Palaeoclimatol. Palaeoecol.* 176, 207–227.
- Stott, L., Cannariato, K., Thunell, R., Haug, G.H., Koutavas, A., Lund, S., 2004. Decline of surface temperature and salinity in the western tropical Pacific Ocean in the Holocene epoch. *Nature* 431, 56–59.
- Talbot, M.R., 1990. A review of the palaeohydrological interpretation of carbon and oxygen isotopic ratios in primary lacustrine carbonates. *Chem. Geol.* 80, 261–279.
- Talbot, M.R., Johannessen, T., 1992. A high resolution palaeoclimatic record for the last 27,500 years in tropical West Africa from the carbon and nitrogen isotopic composition of lacustrine organic matter. *Earth Planet. Sci. Lett.* 110, 23–37.
- Talbot, M.R., Lærdal, T., 2000. The Late Pleistocene-Holocene palaeolimnology of Lake Victoria, East Africa, based upon elemental and isotopic analyses of sedimentary organic matter. *J. Paleolimnol.* 23, 141–164.
- Tan, M., 2014. Circulation effect: response of precipitation $\delta^{18}\text{O}$ to the ENSO cycle in monsoon regions of China. *Clim. Dyn.* 42, 1067–1077.
- Wang, Y.J., Cheng, H., Edwards, R.L., He, Y.Q., Kong, X.G., An, Z.S., Wu, J.Y., Kelly, M.J., Dykoski, A.D., Li, X.D., 2005. The Holocene Asian monsoon: link to solar changes and North Atlantic climate. *Science* 308, 854–857.
- Wen, R.L., Xiao, J.L., Chang, Z.G., Zhai, D.Y., Xu, Q.H., Li, Y.C., Itoh, S., Lomtatidze, Z., 2010. Holocene climate changes in the mid-high-latitude-monsoon margin reflected by the pollen record from Hulun Lake, northeastern Inner Mongolia. *Quat. Res.* 73, 293–303.
- Wen, R.L., Xiao, J.L., Fan, J.W., Zhang, Shengrui, Yamagata, Hideki, 2017. Pollen evidence for a mid-Holocene East Asian summer monsoon maximum in northern China. *Quat. Sci. Rev.* 176, 29–35.
- Xiao, J.L., Fan, J.W., Zhai, D.Y., Wen, R.L., Qin, X.G., 2015. Testing the model for linking grain-size component to lake level status of modern clastic lakes. *Quat. Int.* 355, 34–43.
- Xiao, J.L., Si, B., Zhai, D.Y., Itoh, S., Lomtatidze, Z., 2008. Hydrology of Dali Lake in central-eastern inner Mongolia and Holocene East Asian monsoon variability. *J. Paleolimnol.* 40, 519–528.
- Xiao, J.L., Xu, Q.H., Nakamura, T., Yang, X.L., Liang, W.D., Inouchi, Y., 2004. Holocene vegetation variation in the Daihai Lake region of north-central China: a direct indication of the Asian monsoon climatic history. *Quat. Sci. Rev.* 23, 1669–1679.
- Zhai, D.Y., Xiao, J.L., Zhou, L., Wen, R.L., Chang, Z.G., Pang, Q.Q., 2010. Similar distribution pattern of different phenotypes of *Limnocythere inopinata* (Baird) in a brackish-water lake in Inner Mongolia. *Hydrobiologia* 651, 185–197.
- Zhang, J.F., Xu, B.Q., Turner, F., Zhou, L.P., Gao, P., Lü, X.M., Nesje, A., 2017. Long-term glacier melt fluctuations over the past 2500 yr in monsoonal High Asia revealed by radiocarbon-dated lacustrine pollen concentrates. *Geology* 45, 359–362.
- Zhang, Z.K., Li, G.J., Yan, H., An, Z.S., 2018. Microcodium in Chinese loess as a recorder for the oxygen isotopic composition of monsoonal rainwater. *Quat. Int.* 464, 364–369.
- Zhong, W., Wei, Z.Q., Chen, Y., Shang, S.T., Xue, J.B., Ouyang, J., Cao, J.Y., Chen, B., Zhu, C., 2017. A 15.4-ka paleoclimate record inferred from $\delta^{13}\text{C}$ and $\delta^{15}\text{N}$ of organic matter in sediments from the sub-alpine Daping Swamp, western Nanling Mountains, South China. *J. Paleolimnol.* 57, 127–139.
- Zhou, W.J., Liu, T.B., Wang, H., An, Z.S., Cheng, P., Zhu, Y.Z., Burr, G.S., 2016. Geological record of meltwater events at Qinghai Lake, China from the past 40 ka. *Quat. Sci. Rev.* 149, 279–287.